



Generalized stability landscape of the Atlantic Meridional Overturning Circulation

Matteo Willeit^{1,*} and Andrey Ganopolski^{1,*}

¹Potsdam Institute for Climate Impact Research (PIK), Member of the Leibniz Association, P.O. Box 601203, D-14412 Potsdam Germany

*These authors contributed equally to this work.

Correspondence: Matteo Willeit (willeit@pik-potsdam.de)

Abstract.

The Atlantic Meridional Overturning Circulation (AMOC) plays a crucial role in shaping climate conditions over the North Atlantic region and beyond and its future stability is a matter of concern. While the stability of the AMOC to surface FWF perturbations has been investigated in numerous model simulations, its equilibrium response to changing CO₂ remains largely unexplored and precludes a comprehensive understanding of AMOC stability under ongoing global warming. Here we use a fast Earth system model to explore the stability of the AMOC to combined changes in FWF between -0.25 and +0.25 Sv in the North Atlantic and atmospheric CO₂ concentrations between 180 and 560 ppm. We find four different AMOC states associated with qualitatively different convection patterns in the North Atlantic. Apart from an *Off* AMOC state and a *Modern*-like AMOC with deep water forming in the Labrador and Nordic Seas, we find a *Weak* AMOC state with convection occurring south of 55°N and a *Strong* AMOC state characterized by deep water formation extending into the Arctic. Several of these AMOC states can be stable under the same boundary conditions for specific combinations of CO₂ and FWF. Generally the model shows an increase in equilibrium AMOC strength for higher CO₂ levels. It is also noteworthy that, while under preindustrial conditions the AMOC off state is not stable in the model, it becomes stable for CO₂ concentrations above ~400 ppm, suggesting that an AMOC shutdown in a warmer climate might be irreversible.

1 Introduction

The Atlantic Meridional Overturning Circulation (AMOC) is a critical component of the global climate system and has been extensively studied due to the large climate and societal implications that a change in this circulation would cause in the North Atlantic region, particularly over Europe (Jackson et al., 2015). There is a concern that the AMOC could weaken substantially or even shut down in the future under global warming, and that this could be possibly irreversible due to the existence of multiple equilibrium states (Mecking et al., 2016; Rahmstorf et al., 2005; Manabe and Stouffer, 1988; Jackson and Wood, 2018) in accordance with the seminal work of Stommel (1961), who suggested the presence of multiple stable AMOC states due to the positive salt advection feedback. Stocker and Wright (1991) and Rahmstorf (1995) pioneered the use of surface freshwater forcing (FWF) experiments to analyze the stability of the AMOC and showed a hysteresis behavior in ocean models. Since then, many studies have investigated the response of the AMOC to FWF perturbations in the northern North Atlantic.



25 Models of different complexity have found that the AMOC shows a hysteresis behavior to FWF that is associated with multiple stable states (Ganopolski and Rahmstorf, 2001; Rahmstorf et al., 2005; Hawkins et al., 2011; Hu et al., 2012; van Westen and Dijkstra, 2023; Ando and Oka, 2021; Hofmann and Rahmstorf, 2009; Gregory et al., 2003; Lenton et al., 2009), although there is no consensus as to whether the AMOC is in a monostable or a bistable regime under present climate conditions. While most of these experiments have been performed under pre-industrial or present-day conditions, some have considered the dependence on background climate by exploring the hysteresis behavior also for the last glacial maximum (Ganopolski and Rahmstorf, 2001; Schmittner et al., 2002; Ando and Oka, 2021; Pöppelmeier et al., 2021). Most of the hysteresis experiments have been performed with FWF in the latitudinal belt between 20–50°N in the Atlantic, thereby avoiding a direct perturbation of the convection sites further north in order to focus on the salt-advection feedback. The AMOC stability to FWF at higher latitudes (e.g. 50–70°N), where convection and deep water formation take place, has received comparatively less attention. FWF applied in the convection areas has a stronger impact on the AMOC (e.g. Ganopolski and Rahmstorf, 2001), because the state of the AMOC is tightly linked to the production of deep water. However, convection is controlled by the surface buoyancy flux, which does not only depend on FWF, but also on the sensible heat cooling and the temperature at the sea surface. The temperature dependence of the surface buoyancy flux arises from the nonlinear equation of state of seawater, and in particular from the temperature dependence of the thermal expansion coefficient (e.g. Roquet et al., 2015). The effect of temperature on AMOC stability has been only marginally investigated (e.g. Hu et al., 2023; Gérard and Crucifix, 2024), but could be crucial in determining AMOC stability in a changing climate. Here we use an Earth system model to explore the combined effect of surface FWF and temperature on AMOC stability. The effect of FWF is quantified by running experiments with FWF in different latitudinal belts in the North Atlantic, while the effect of temperature is explored by varying the atmospheric CO₂ concentration, which is one of the main factors driving past and future climate changes.

45 **2 AMOC hysteresis in freshwater space**

A common approach to investigate the stability of the AMOC has historically been to apply perturbations in the surface freshwater balance of the North Atlantic (Stocker and Wright, 1991; Rahmstorf, 1995). We used the fast Earth system model CLIMBER-X (Willeit et al., 2022) to perform standard FWF experiments to track the stable states of the AMOC. CLIMBER-X has a horizontal resolution of 5°x5° in the atmosphere, ocean, sea ice and land components and 23 unequally-spaced vertical layers in the ocean (see Appendix A1) and has been shown to perform well both in terms of present-day simulated climate and in terms of sensitivities to different forcings and changes in boundary conditions Willeit et al. (2022). Notably, the model has recently been shown to reproduce Dansgaard-Oeschger events under mid-glacial conditions (Willeit et al., 2024), further confirming that it is a suitable tool to study AMOC stability. CLIMBER-X is a computationally efficient model that allows to perform the long simulations required for a comprehensive stability analysis of the AMOC.

55 When driven by slowly varying changes in the FWF in different latitudinal belts in the North Atlantic (see Appendix A2), CLIMBER-X shows the typical hysteresis behaviour (Fig. 1) seen also in a hierarchy of other models of varying complexity (Ganopolski and Rahmstorf, 2001; Rahmstorf et al., 2005; Hawkins et al., 2011; Hu et al., 2012; van Westen and Dijkstra,

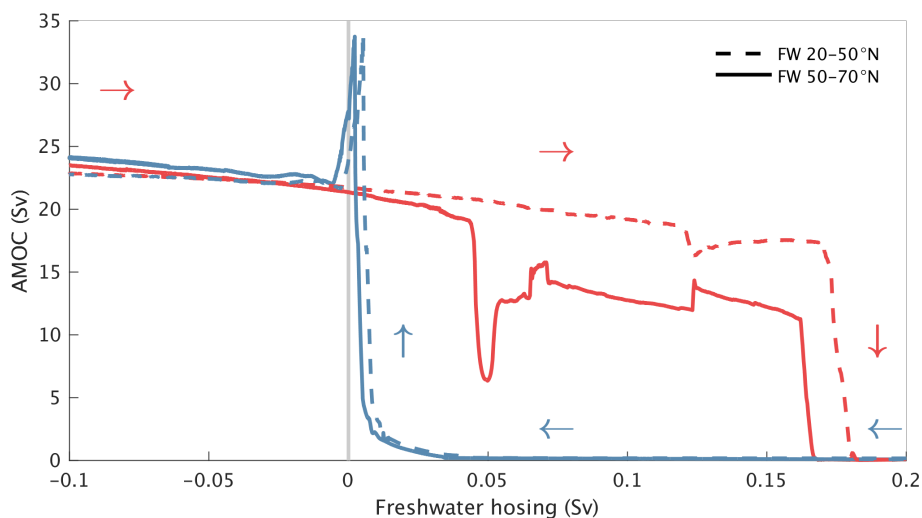


Figure 1. Hysteresis of the AMOC in freshwater space. AMOC response to prescribed changes in FWF in two different latitudinal belts in the North Atlantic (dashed lines for 20–50°N and solid lines for 50–70°N). The red lines are from simulations with increasing FWF starting at -0.5 Sv and the blue lines are for experiments with decreasing FWF starting at +0.5 Sv. In all cases the rate of change of the imposed FWF is 0.02 Sv kyr^{-1} , so that each full simulation covering the FWF range between -0.5 Sv to +0.5 Sv (only partly shown in the figure) corresponds to 50,000 simulation years.

2023; Ando and Oka, 2021; Hofmann and Rahmstorf, 2009; Gérard and Crucifix, 2024). In particular there is a range of FWF over which the AMOC has two stable states. The AMOC in the model is monostable under pre-industrial conditions, although relatively close to bi-stability. The hysteresis is wider if FWF is applied between 20–50°N compared to when it is applied to the latitudinal belt 50–70°N, where convection occurs (Fig. 1). When FWF is increased under pre-industrial conditions, a critical point is reached where the AMOC shows a rather abrupt (both in FWF space and in time) weakening, suggesting a prominent role of convective instability as opposed to the expected parabolic shape resulting from a Stommel-like bifurcation (Stommel, 1961). The AMOC is more sensitive to FWF perturbations applied between 50°N and 70°N, in which case an abrupt weakening of the AMOC occurs already for a hosing of $\sim 0.05 \text{ Sv}$ (Fig. 1). This is the result of a collapse of deepwater formation in the Labrador and Irminger Seas and a general shift of the convection to latitudes south of $\sim 55^\circ\text{N}$, resembling Stadal-like conditions of observed past Dansgaard-Oeschger events. It should be noted that this *Weak* AMOC state is seen only in the experiments with FWF hosing applied directly to the convection regions between 50°N and 70°N, while most AMOC hysteresis experiments to date have been performed with FWF at lower latitudes (usually between 20°N and 50°N). A complete AMOC shutdown occurs for FWF of $\sim 0.17\text{-}0.18 \text{ Sv}$, depending on the latitude of the applied forcing (Fig. 1).

In our hysteresis experiments we applied a very slow rate of change of $0.02 \text{ Sv per } 1000 \text{ years}$ in the FWF. When repeating the experiment with a ten times higher rate of change (0.2 Sv kyr^{-1}), a value typically used in computationally expensive state-of-the-art climate models (e.g. van Westen and Dijkstra, 2023; Hu et al., 2012), the hysteresis looks very different (Fig. B1). For a higher rate of change in the forcing, the hysteresis is generally smoother and more regular and does not show the abrupt



75 transitions that characterize the hysteresis curves produced with slow FWF changes. Notably, the *Weak* AMOC mode is not
captured in the fast hysteresis experiments, where the AMOC is gradually transitioning to an *Off* state when the FWF exceeds
 $\sim 0.05 \text{ Sv}$ (Fig. B1b). In the experiments with decreasing FWF the higher forcing rate leads to a much delayed recovery of the
AMOC from the *Off* state, resulting in a very distorted representation of the bistability range. In particular, the slow forcing
experiments show that the AMOC is monostable under pre-industrial conditions in our model, while the fast forcing simulations
80 give the wrong impression that the AMOC *Off* state is also stable (Fig. B1).

3 Equilibrium AMOC response to CO₂ changes

Another way of looking at AMOC stability, which is possibly more relevant for the ongoing global warming, is to investigate
the AMOC response to changes in atmospheric CO₂. In an experiment where the CO₂ concentration is very slowly increased
starting from 180 ppm up to 560 ppm ($0.002 \% \text{ yr}^{-1}$ see also Appendix A2), the model shows a general increase in AMOC
85 strength with increasing global temperature under quasi-equilibrium conditions (Fig. 2, red line). A weaker AMOC for CO₂
concentrations lower than pre-industrial has been found also in general circulation models (Stouffer and Manabe, 2003; Oka
et al., 2012, 2021; Brown and Galbraith, 2016; Galbraith and de Lavergne, 2019; Klockmann et al., 2018). Stouffer and
Manabe (2003) found AMOC strengthening under doubling and quadrupling of CO₂ relative to pre-industrial levels, and
recently Bonan et al. (2022) showed that at least some state-of-the-art climate models produce an AMOC that is appreciably
90 stronger under CO₂ quadrupling. Gérard and Crucifix (2024) recently analyzed the AMOC response to a slow CO₂ increase
and found a gradual AMOC weakening and eventual collapse at CO₂ above $\sim 1500 \text{ ppm}$. However, their rate of change of
CO₂ of 0.14 ppm yr^{-1} is much larger than the rate that we use in this study ($\sim 0.005 \text{ ppm yr}^{-1}$) and it has been shown that
the AMOC response is highly sensitive to the applied rate of temperature change (Stocker and Schmittner, 1997).

The general AMOC strengthening with warming in the model is punctuated by two discrete transitions at $\sim 250 \text{ ppm}$ and
95 $\sim 370 \text{ ppm}$ (Fig. 2), separating three different AMOC states and convection patterns in the North Atlantic (Fig. 3). The warmer
the climate the further north do the sites of deepwater formation shift, following the northward retreat of sea ice (Fig. 3b-d), and
the stronger and deeper the simulated AMOC is (Fig. 3f-h). A few general circulation models found thermal AMOC thresholds
under climate conditions generally colder than the pre-industrial, leading to abrupt AMOC weakening when climate is cooled
and abrupt AMOC strengthening when climate is warmed (Knorr and Lohmann, 2007; Oka et al., 2012; Zhang et al., 2017;
100 Banderas et al., 2012). Adloff (2023) also found several thermal thresholds in the AMOC in idealized simulations of the last
glacial cycle.

Willeit et al. (2024) have shown that around the transition between a *Modern* and *Weak* AMOC at $\sim 250 \text{ ppm}$ CLIMBER-X
simulates Dansgaard-Oeschger-like events in the presence of noise. This millennial-scale variability originates from internal
climate system dynamics associated with transitions between two distinct convection patterns that are stable for different CO₂
105 concentrations. For CO₂ above $\sim 250 \text{ ppm}$, the convection pattern resembles the present-day state with deep water forming in
the Labrador Sea and in the Nordic Seas (Fig. 3c), while for CO₂ below $\sim 250 \text{ ppm}$ convection can not be sustained in the
Labrador and Irminger Seas and is generally restricted to areas south of $\sim 55^\circ \text{N}$ (Fig. 3b). This state is equivalent to the *Weak*

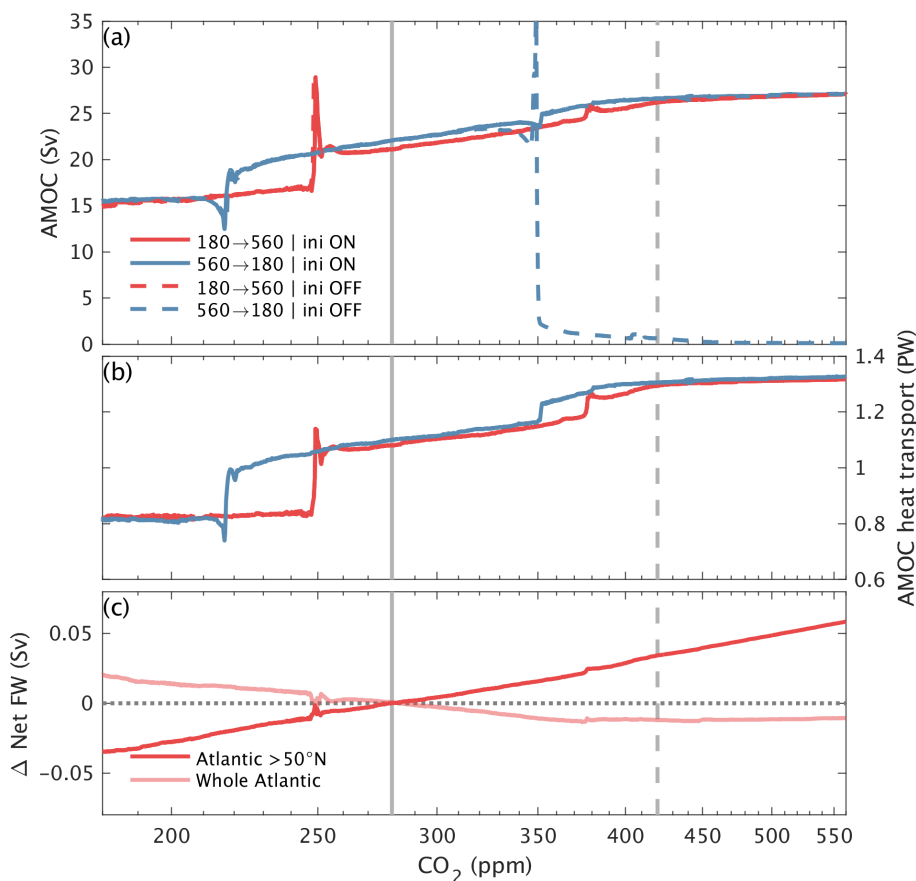


Figure 2. Quasi-equilibrium AMOC response to changes in CO_2 . (a) Maximum of the AMOC streamfunction, (b) maximum meridional heat transport by the ocean in the Atlantic and (c) changes in net surface freshwater flux in the Atlantic in simulations with slowly varying prescribed atmospheric CO_2 concentrations for CO_2 increasing from 180 ppm (red lines) and for CO_2 decreasing from 560 ppm (blue lines). The solid lines are from simulations initialized from a pre-industrial AMOC state, while the dashed lines are from simulations initialized from the AMOC off state. In (b) and (c) only selected simulations are shown. The solid vertical line indicates the pre-industrial CO_2 concentration of 280 ppm and the dashed vertical line shows the present-day (2024 CE) CO_2 concentration.

AMOC state in Fig. 1. A narrow window of CO_2 concentrations exists for which both convection patterns are stable for the same CO_2 (Fig. 2, red vs blue solid lines), but this has been shown to not be a requirement for the existence of millennial-scale variability (Willeit et al., 2024). It should be noted that in the past CO_2 concentrations below the pre-industrial level of 280 ppm were related to the appearance of large continental ice sheets over the NH, which affect AMOC stability (e.g. Zhang et al., 2014; Klockmann et al., 2018; Willeit et al., 2024) but are not considered in the present study.

The AMOC transition at ~ 370 ppm is associated with a convection start in the Kara Sea and Nansen Basin (Fig. 3c), and has a clearer imprint in the Atlantic meridional heat transport (Fig. 2b) than in the maximum strength of the the AMOC (Fig. 2a). We term this the *Strong* AMOC state. Convection in the Arctic is triggered in several climate models in response to future

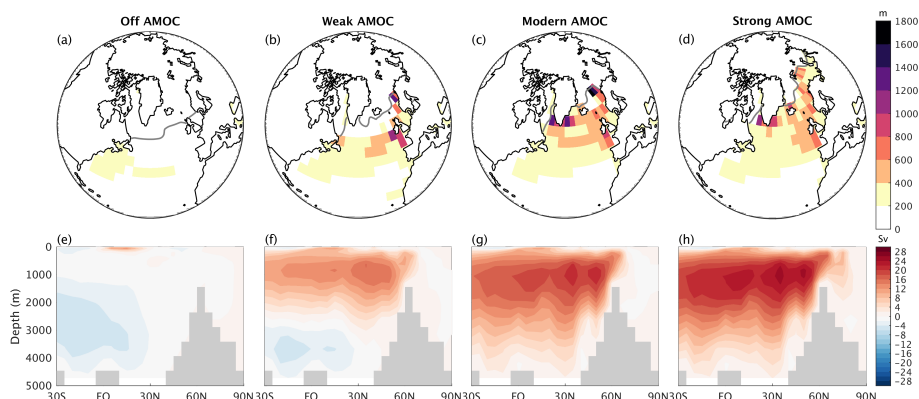


Figure 3. The different AMOC states. (a-d) Seasonal maximum mixed layer depth and (e-h) AMOC streamfunction for the different equilibrium AMOC states in the model: (a,e) *Off*, (b,f) *Weak*, (c,g) *Modern* and (d,h) *Strong* AMOC states. The grey line in (a-d) shows the seasonal maximum sea ice extent (defined as sea ice concentration >0.15).

transient global warming (Brodeau and Koenig, 2016; Bretones et al., 2022; Lique et al., 2018; Lique and Thomas, 2018; Pan et al., 2023), although in many other models this does not occur (Heuzé and Liu, 2024). However, the fact that convection in the Arctic in some models starts even in transient simulations that are characterized by an overall weakening of the AMOC, suggests that the Arctic would be a plausible new location of deep water formation in a warmer climate under quasi-equilibrium conditions.

Model simulations initialized at 180 ppm with an *Off* AMOC state (see Appendix A2) (Fig. 2a, dashed red line) indicate that the AMOC *Off* state is not stable for CO_2 concentrations below pre-industrial levels, resulting in a monostable AMOC for pre-industrial conditions in our model (excluding the relatively narrow hysteresis around the transition at ~ 250 ppm). However if the model is initialized in an AMOC *Off* state at 560 ppm the AMOC remains in the *Off* state as long as CO_2 decreases to values below ~ 350 ppm, after which the AMOC recovers with an overshoot (Fig. 2a, dashed blue line). Our model has therefore two widely different stable AMOC states for CO_2 concentrations above ~ 350 ppm, the AMOC *Off* state and a *Strong* state characterized by a more vigorous AMOC than at present (Fig. 2a). Hu et al. (2023) performed a similar AMOC hysteresis analysis using future climate scenarios, and found that the AMOC exhibits two stable states for CO_2 concentrations ~ 1000 ppm in their model.

It is interesting to note that the AMOC strengthening with global warming occurs despite an associated increase in the net freshwater flux into the northern North Atlantic, north of 50°N (Fig. 2c). This is a result of an intensification of the hydrological cycle in a warming climate, with the typical wet-gets-wetter and dry-gets-drier pattern (Held and Soden, 2006; Zhang et al., 2013). For CO_2 doubling the net freshwater flux into the northern North Atlantic increases by ~ 0.07 Sv, an amount which is sufficient to cause a transition of the AMOC into a weak state if CO_2 is kept constant at pre-industrial values, as shown in Fig. 1. 0.07 Sv is a relative large freshwater flux, which is an order of magnitude higher than the net freshwater flux from the Greenland ice sheet simulated under similar temperatures (Calov et al., 2018), and would roughly correspond to the rate of



freshwater input resulting from the Greenland ice sheet melting completely over a time period of ~ 1500 years. The increase in freshwater at high latitudes in the Atlantic as a response to global warming is a consistent feature also of CMIP6 models under transient future scenarios (Fig. B2a). While the northern North Atlantic gets wetter as climate warms, in the model the net surface freshwater flux into the whole Atlantic Ocean shows the opposite trend, with a small decrease in net freshwater flux as CO_2 concentrations increase (Fig. 2c). Most CMIP6 models show a larger decrease of the net freshwater flux into the Atlantic than CLIMBER-X as climate warms (Fig. B2b), but with a relatively wide spread between models.

The effect of changes in the net surface freshwater flux associated with global warming on AMOC stability is therefore the result of a stabilizing effect due to salinification of the Atlantic as a whole, which stabilizes the AMOC through the salt-advection feedback, and the freshening of the northern Atlantic region, which destabilizes the AMOC through an increased surface buoyancy flux and a consequent lowering of the surface seawater density in the deep-water formation regions.

4 AMOC stability landscape in combined CO_2 and freshwater space

The above analyses of the response of the AMOC to changes in FWF and atmospheric CO_2 have shown that there are at least four different stable AMOC states in CLIMBER-X, namely *Off*, *Weak*, *Modern* and *Strong*. The CO_2 –freshwater conditions under which these different AMOC states are stable can be investigated by tracing their stability through the CO_2 –FWF space. This is done by following the CO_2 –FWF paths illustrated in Fig. A1 as described in detail in Appendix A2. The results are shown separately for each AMOC state in Fig. 4. High CO_2 and low FWF generally favor stronger AMOC states (Fig. 4 and Fig. 5). The *Strong* AMOC state is characteristic of climates warmer than pre-industrial (Fig. 4d). As seen already in Fig. 2, without FWF the AMOC transitions to the *Strong* state for CO_2 concentrations above ~ 380 ppm. The *Modern* AMOC state covers conditions going from low CO_2 and negative FWF to high CO_2 and FWF up to 0.1 Sv , passing through pre-industrial conditions (Fig. 4c). If the climate would be in equilibrium with present-day CO_2 concentrations of ~ 420 ppm, the model suggests that the *Modern* AMOC state would not be stable, but that the AMOC would rather be in the *Strong* state instead (Fig. 4c,d). The *Weak* AMOC state exists for a range of CO_2 concentrations between ~ 200 and ~ 560 ppm and FWF roughly between -0.05 and 0.18 Sv (Fig. 4b). Starting from pre-industrial conditions the *Weak* AMOC state can be reached either by reducing CO_2 or by adding freshwater to the North Atlantic, north of 50°N , as shown also in Fig. 2a,b and Fig. 1. For the investigated range of CO_2 concentrations an *Off* AMOC state can not be achieved by varying CO_2 alone, but only through a large enough FWF. Under quasi-equilibrium conditions, the FWF needed to shut down the AMOC when starting from an 'on' AMOC state is in the range ~ 0.05 – 0.2 Sv , depending on the CO_2 concentration (Fig. 4b and Fig. 5). If the FWF is larger than $\sim 0.05 \text{ Sv}$, the *Off* AMOC state is stable for any CO_2 concentration (Fig. 4a). For smaller or negative FWF the stability of the *Off* state depends on CO_2 . The AMOC bistability range generally broadens with warming (Fig. 5), particularly because the AMOC recovery from the *Off* state requires an increasingly more negative FWF (Fig. 4a). In the model the *Off* state is not stable under pre-industrial conditions, but it is for present-day CO_2 concentrations (Fig. 4a).

We use the remarkable fact that all four AMOC states in the model are stable under the same boundary conditions for CO_2 concentrations ~ 440 ppm and FWF $\sim 0.05 \text{ Sv}$ (Fig. 5) to explore the pure effect of the different AMOC states on climate. An

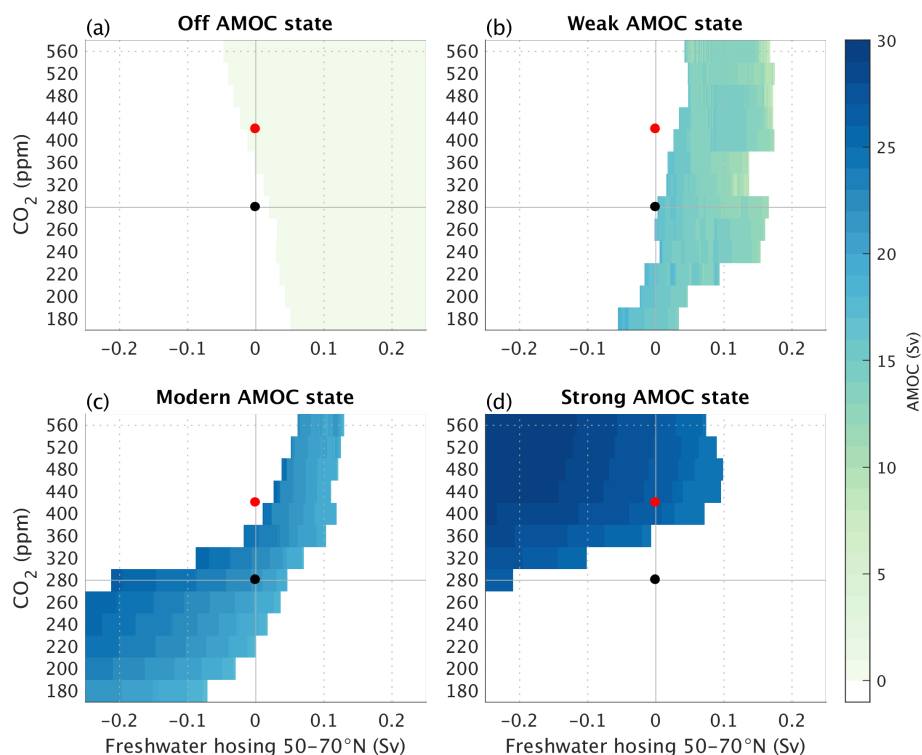


Figure 4. AMOC states in combined CO_2 and freshwater space. Maximum of the AMOC streamfunction as a function of CO_2 and FWF between $50\text{--}70^\circ\text{N}$ separately for the four different stable AMOC states in the model, namely (a) *Off* AMOC state, (b) *Weak* AMOC state, (c) *Modern* AMOC state and (d) *Strong* AMOC state. The black dot indicates pre-industrial conditions, while the red dot marks the current atmospheric CO_2 concentration. The stability landscape is constructed based on simulations following the paths shown in Fig. A1, where the rate of change of CO_2 is $0.002\% \text{ yr}^{-1}$ as in Fig. 2 and the rate of change of FWF is 0.02 Sv kyr^{-1} as in Fig. 1.

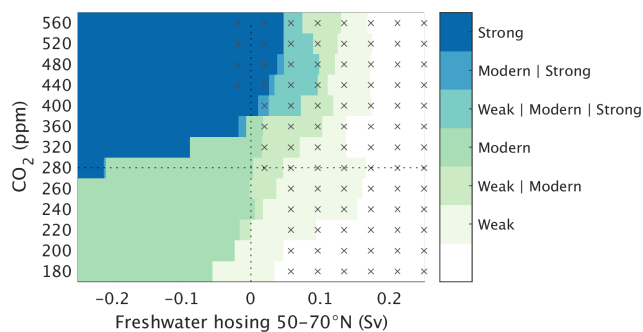


Figure 5. Summary of AMOC stability landscape in combined CO_2 and freshwater space. The colored regions indicate the on AMOC states that are stable under the given CO_2 and FWF as indicated in the legend. The crosses indicate the area where the *Off* AMOC state is stable. Note that multiple AMOC states are stable under some boundary conditions.

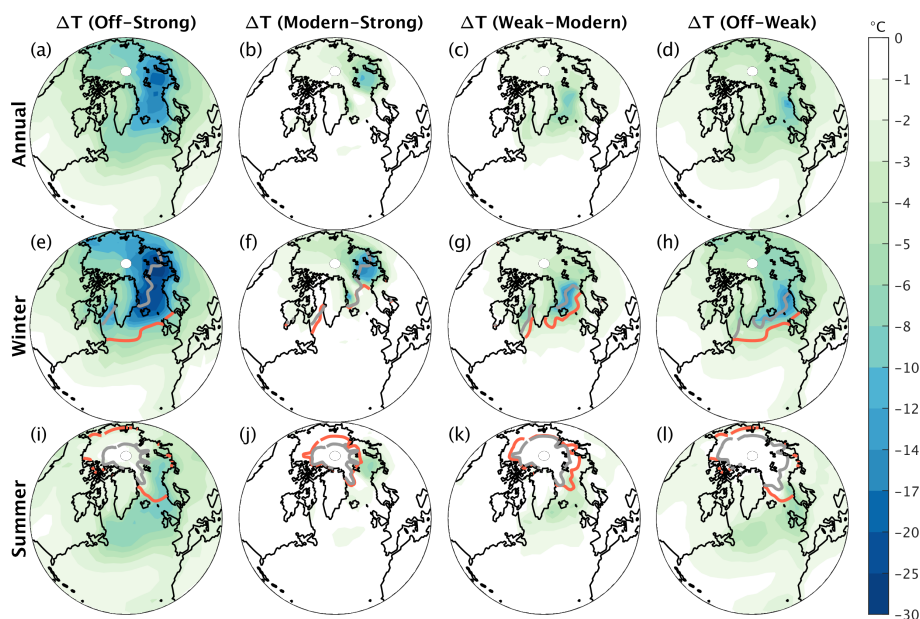


Figure 6. Temperature differences induced by different AMOC states. (a-d) Annual, (e-h) winter (December-January-February) and (i-l) summer (June-July-August) temperature differences between different AMOC states as indicated in the panels. The colored lines show the seasonal maximum sea ice extent in (e-h) and the seasonal minimum sea ice extent in (i-l), with the grey line always corresponding to the stronger AMOC state and the orange line to the weaker AMOC state. Sea ice extent is defined as sea ice concentration >0.15.

170 AMOC weakening generally causes a cooling that is most pronounced in the northern North Atlantic, but that also extends more widely to the mid- to high-latitudes of the Northern Hemisphere (Fig. 6), with the largest effect being observed in winter (Fig. 6e-h) and the weakest in summer (Fig. 6i-l). This is in general agreement with previous studies looking at the climate impact of an AMOC shutdown forced by FWF (e.g. van Westen and Dijkstra, 2023; Jackson et al., 2015). The largest possible effect of AMOC on climate is for a transition between the *Strong* and *Off* states (Fig. 6a,e,i), which shows an annual mean

175 cooling of up to 20°C in the northern North Atlantic, with temperatures as much as ~25-30°C colder in winter, associated also with a pronounced sea ice advance (Fig. 6e). A shift from *Strong* to *Modern* AMOC induces a cooling of ~10°C in the Barents and Kara Seas (Fig. 6b,f,j), while a transition from *Modern* to *Weak* AMOC mainly affects the Nordic Seas with a cooling of ~15°C in winter (Fig. 6c,g,k). A shift from a *Weak* to an *Off* AMOC state has a strong imprint on temperatures in the Nordic Seas and the Labrador and Irminger Seas (Fig. 6d,h,l). In general, the differences in climate between the different

180 AMOC states are related to the shifts in the location of deep water formation in the North Atlantic and the associated changes in sea ice extent (Fig. 3a-d).



5 Discussion and Conclusions

For the first time, we have performed a systematic analysis of the AMOC stability in the FWF–CO₂ space. This was done by very slowly varying the surface freshwater flux in the North Atlantic and the atmospheric CO₂ concentration and required
185 ~1,000,000 model years of simulation.

We found four distinct modes of the AMOC. Apart from the *Modern* and the *Off* AMOC states, we find two additional equilibrium states: (i) a *Weak*, Stadial-like, AMOC state with deep water forming predominantly south of ~55°N for CO₂ below ~250 ppm or FWF in the latitudinal belt 50–70°N above ~0.05 Sv, (ii) a *Strong* AMOC state with convection reaching into the Arctic for CO₂ above ~350 ppm or FWF in the latitudinal belt 50–70°N below ~-0.2 Sv. Intermediate stable AMOC
190 states between *Modern* and *Off* associated with changes in the convection pattern have also been found in previous studies (Rahmstorf, 1995; Lohmann et al., 2024) using ocean-only models forced with increasing FWF, but our results indicate that the standard method of tracing hysteresis in the FWF space may not be enough to find all possible AMOC modes.

Our AMOC stability landscape explains why warm climates are generally stable and cold are unstable. The fact that the AMOC is monostable under pre-industrial-like conditions explains why the AMOC always recovered at the end of glacial
195 terminations. The existence of the *Weak* AMOC state has been shown by Willeit et al. (2024) to be related to Dansgaard-Oeschger events in the model. Our results suggest that a different mode of AMOC (the *Strong* mode) was possible during past warm and stable climate conditions, such as the Pliocene (e.g. Zhang et al., 2021; Weiffenbach et al., 2023). Whether the existence of the *Strong* AMOC state could potentially lead to some kind of centennial or millennial-scale variability in the AMOC in a warmer climate remains to be explored.

Our results indicate a generally stronger and deeper AMOC at equilibrium under warmer climate conditions. This is in contrast to the projected AMOC weakening response to anthropogenic global warming (e.g. Weijer et al., 2020; Weaver et al., 2012), which is an intrinsically transient response of the system predominantly induced by the rapid temperature increase (Gregory et al., 2005; Weaver et al., 2007; Levang and Schmitt, 2020). In the phase space, a CO₂ increase drives the AMOC away from the tipping point towards a stronger and more stable AMOC. This is because the AMOC response to CO₂ is funda-
205 mentally different from the response to FWF. In the case of FWF, regardless of the rate of change, an increase in FWF weakens the AMOC. In the case of CO₂, this is not true: a fast enough increase in CO₂ weakens the AMOC (Stocker and Schmittner, 1997), while a very slow (quasi-equilibrium) increase strengthens it. Since the main cause of future AMOC weakening is the increase in CO₂, the traditional FWF hysteresis analysis is of limited use for predicting the future AMOC evolution.

Even if our stability diagram can not explain the AMOC response to transient CO₂ forcing, it provides some information
210 on whether the transient weakening of the AMOC is reversible (mono-stable regime) or irreversible (bi-stable). Our results suggest that a future AMOC shutdown, which could be triggered by the transient response to anthropogenic global warming, could be irreversible because the *Off* AMOC state is stable for CO₂ concentrations above the present-day level. Our model simulations therefore indicate that in terms of stability landscape the AMOC is currently moving towards a stronger state, but from a monostable into a bistable regime, where the AMOC *Off* state is also stable.



215 It should be noted that the AMOC stability landscape presented above is a result of model simulations with the fast Earth
system model CLIMBER-X, which has a relatively coarse-resolution and whose ocean model is based on the quasi-geostrophic
approximation, with all the attendant limitations. Generally, anything related to convection and changes in convective patterns
is highly model dependent, with widely different results produced even among state-of-the-art general circulation models
(Sgubin et al., 2017; Heuzé, 2017; Treguier et al., 2023). However, since the experiments presented in the paper can only be
220 performed with a model like CLIMBER-X, we believe that they are useful to illustrate the general concept of AMOC stability.
Also, since CLIMBER-X does not produce internal interannual climate variability it is possible that different modes of the
AMOC, which are distinct in our simulations, may not be distinguished in the presence of strong variability. Obviously, this
does not question the existence of distinct Stadial and Interstadial AMOC modes during glacial times.

Code and data availability. The CLIMBER-X model is freely available as open source code at <https://zenodo.org/record/7898797>.

225 **Appendix A: Materials and Methods**

A1 Earth System Model

We use the CLIMBER-X Earth system model (Willeit et al., 2022) in a climate-only setup, including the frictional-geostrophic
3D ocean model GOLDSTEIN (Edwards et al., 1998; Edwards and Marsh, 2005) with 23 vertical layers, the semi-empirical
statistical-dynamical atmosphere model SESAM (Willeit et al., 2022), the dynamic-thermodynamic sea ice model SISIM
230 (Willeit et al., 2022) and the land surface model with interactive vegetation PALADYN (Willeit and Ganopolski, 2016). All
components of the climate model have a horizontal resolution of $5^\circ \times 5^\circ$. The model is open source, is described in detail in
Willeit et al. (2022) and in general shows performances that are comparable with state-of-the-art CMIP6 models under different
forcings and boundary conditions.

A2 Experiments

235 With CLIMBER-X we run transient simulations where we slowly varied either the FWF in the North Atlantic or the atmo-
spheric CO_2 concentration.

The standard FWF experiments were performed with prescribed changes in freshwater flux with a rate of $\pm 0.02 \text{ Sv kyr}^{-1}$
in two different latitudinal belts, $20\text{--}50^\circ\text{N}$ and $50\text{--}70^\circ\text{N}$ in the North Atlantic, either starting from an initial hosing flux of
 -0.5 Sv and slowly increasing it until 0.5 Sv , or starting from $+0.5 \text{ Sv}$ hosing flux and gradually decreasing it until -0.5 Sv .
240 Each simulation is 50,000 years long. These two experiments were performed with prescribed constant CO_2 concentration of
280 ppm. The initial condition for both these experiments is a pre-industrial equilibrium simulation run for 10000 years with
280 ppm of CO_2 and present-day ice sheets. To investigate how the rate of change of the FWF affects the hysteresis behaviour,

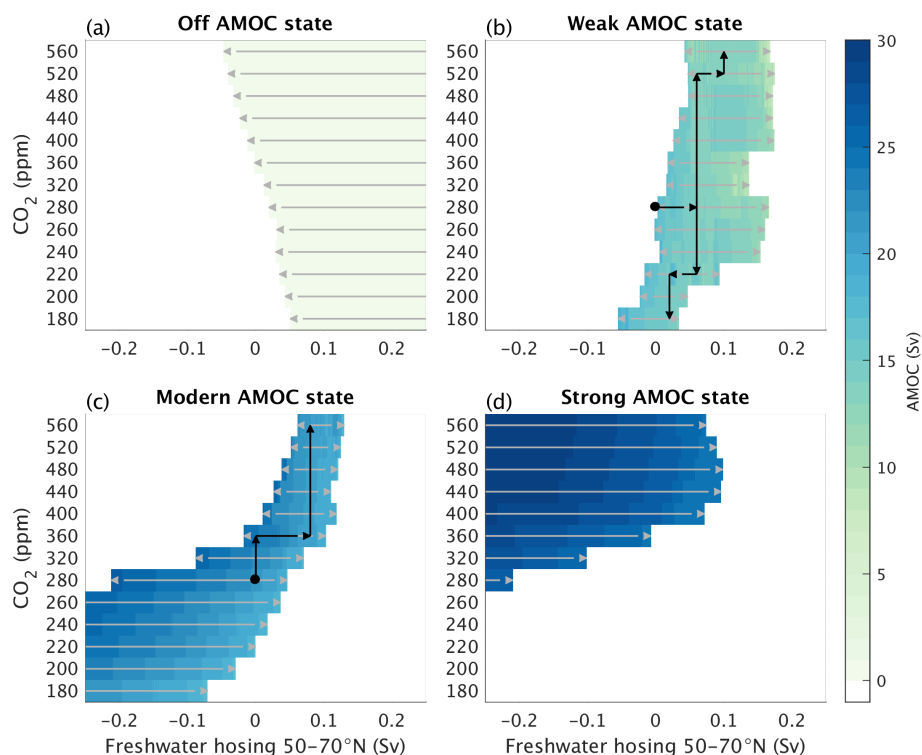


Figure A1. Simulation pathways used to explore the stability of the four different AMOC states in the combined CO₂ and freshwater space.

we also repeated the freshwater hysteresis analysis using a 10× faster rate of change of the FWF (0.2 Sv kyr⁻¹) and a slower rate of change of 0.005 Sv kyr⁻¹.

245 We additionally performed transient simulations with slowly varying CO₂ concentrations: (i) starting at 180 ppm and gradually increasing CO₂ up to 560 ppm and (ii) starting from 560 ppm and gradually decreasing CO₂ down to 180 ppm. In both cases the rate of change of CO₂ is 2 % kyr⁻¹ implying a total simulation length of ~56,500 years. The initial state for these simulations is a 10,000 years long equilibrium run with either 180 ppm (for (i)) or 560 ppm (for (ii)) of atmospheric CO₂. Simulations (i) and (ii) are also repeated using initial states where the AMOC is forced to be in the off state. The 180 ppm and
250 560 ppm initial states with AMOC off are obtained by prescribing 0.2 Sv of FWF in the latitudinal belt 50–70°N in the North Atlantic and running the model for 5000 years.

To investigate the stability of the four different AMOC states found from the FWF and CO₂ perturbation experiments above in a combined FWF–CO₂ space, we interactively designed simulation pathways through this parameter space as shown in Fig. A1. The rate of change of the forcing in these experiments is again 0.02 Sv kyr⁻¹ for FWF and 2 % kyr⁻¹ for CO₂. The
255 constant CO₂ concentrations used to move in the FWF direction are discretized in steps of 20 ppm between 180 ppm and 280 ppm and in steps of 40 ppm between 280 ppm and 560 ppm.

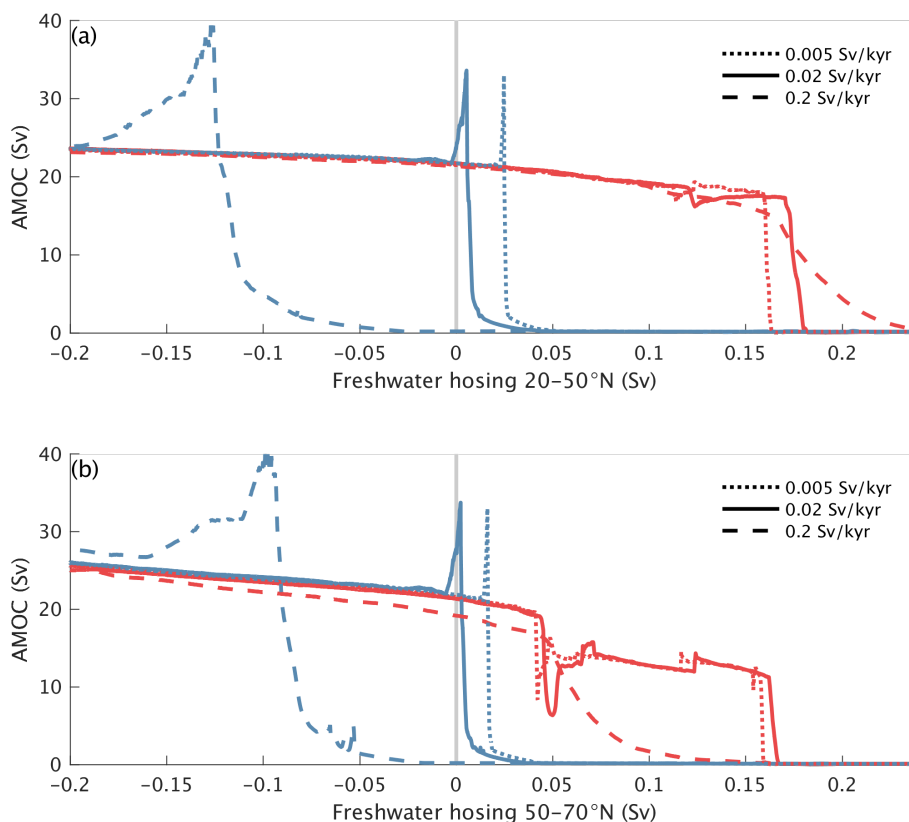


Figure B1. Rate-dependence of the hysteresis of the AMOC in freshwater space. AMOC response to prescribed changes in FWF in the latitudinal belts (a) 20–50°N and (b) 50–70°N. The red lines are from simulations with increasing FWF starting at -0.5 Sv and the blue lines are for experiments with decreasing FWF starting at +0.5 Sv. The continuous lines are with the reference rate of change of the imposed FWF of 0.02 Sv kyr⁻¹ as also shown in Fig. 1, while the dashed lines represent simulations with a ten-fold increase in the rate of change of hosing (0.2 Sv kyr⁻¹) and the dotted lines are for simulations with an even slower rate of change of 0.005 Sv kyr⁻¹.

Appendix B: Additional figures

Author contributions. MW and AG conceived and designed the study. MW performed the model simulations and created the figures. MW and AG wrote the paper.

260 *Competing interests.* The authors declare that they have no conflict of interest.

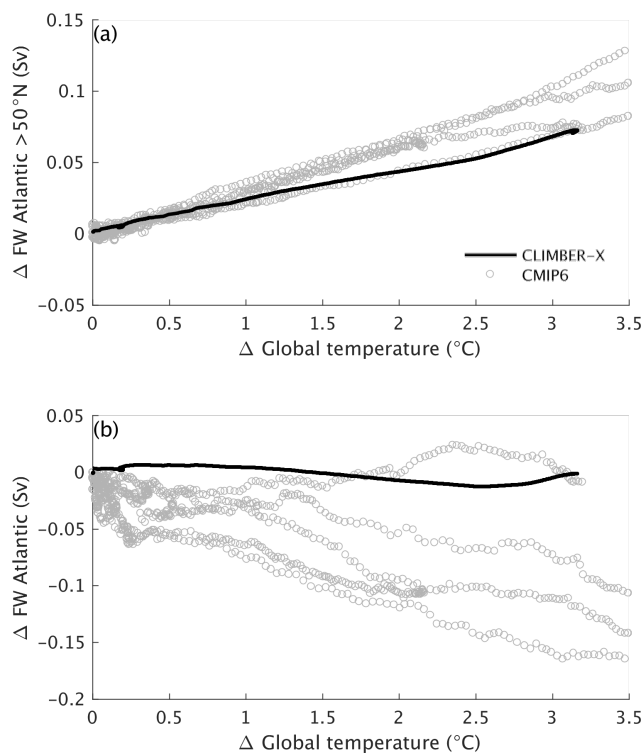


Figure B2.

Acknowledgements. MW is funded by the German climate modeling project PalMod supported by the German Federal Ministry of Education and Research (BMBF) as a Research for Sustainability initiative (FONA) (grant nos. 01LP1920B, 01LP1917D, 01LP2305B). The authors gratefully acknowledge the European Regional Development Fund (ERDF), the German Federal Ministry of Education and Research and the Land Brandenburg for supporting this project by providing resources on the high performance computer system at the Potsdam Institute

265 for Climate Impact Research.



References

- Adloff, M.: Multiple thermal AMOC thresholds in the intermediate complexity model Bern3D, *Climate of the Past - Discussions*, pp. 1–33, <https://doi.org/10.5194/cp-2023-82>, 2023.
- Ando, T. and Oka, A.: Hysteresis of the Glacial Atlantic Meridional Overturning Circulation Controlled by Thermal Feedbacks, *Geophysical Research Letters*, 48, 1–9, <https://doi.org/10.1029/2021GL095809>, 2021.
- 270 Banderas, R., Álvarez-Solas, J., and Montoya, M.: Role of CO₂ and Southern Ocean winds in glacial abrupt climate change, *Climate of the Past*, 8, 1011–1021, <https://doi.org/10.5194/cp-8-1011-2012>, 2012.
- Bonan, D. B., Thompson, A. F., Newsom, E. R., Sun, S., and Rugenstein, M.: Transient and Equilibrium Responses of the Atlantic Overturning Circulation to Warming in Coupled Climate Models: The Role of Temperature and Salinity, *Journal of Climate*, 35, 5173–5193, <https://doi.org/10.1175/JCLI-D-21-0912.1>, 2022.
- 275 Bretones, A., Nisancioglu, K. H., Jensen, M. F., Brakstad, A., and Yang, S.: Transient Increase in Arctic Deep-Water Formation and Ocean Circulation under Sea Ice Retreat, *Journal of Climate*, 35, 109–124, <https://doi.org/10.1175/JCLI-D-21-0152.1>, 2022.
- Brodeau, L. and Koenigk, T.: Extinction of the northern oceanic deep convection in an ensemble of climate model simulations of the 20th and 21st centuries, *Climate Dynamics*, 46, 2863–2882, <https://doi.org/10.1007/s00382-015-2736-5>, 2016.
- 280 Brown, N. and Galbraith, E. D.: Hosed vs. unhosed: Interruptions of the Atlantic Meridional Overturning Circulation in a global coupled model, with and without freshwater forcing, *Climate of the Past*, 12, 1663–1679, <https://doi.org/10.5194/cp-12-1663-2016>, 2016.
- Calov, R., Beyer, S., Greve, R., Beckmann, J., Willeit, M., Kleiner, T., Rückamp, M., Humbert, A., and Ganopolski, A.: Simulation of the future sea level contribution of Greenland with a new glacial system model, *Cryosphere*, 12, 3097–3121, <https://doi.org/10.5194/tc-12-3097-2018>, 2018.
- 285 Edwards, N. R. and Marsh, R.: Uncertainties due to transport-parameter sensitivity in an efficient 3-D ocean-climate model, *Climate Dynamics*, 24, 415–433, <https://doi.org/10.1007/s00382-004-0508-8>, 2005.
- Edwards, N. R., Willmott, A. J., and Killworth, P. D.: On the Role of Topography and Wind Stress on the Stability of the Thermohaline Circulation, *Journal of Physical Oceanography*, 28, 756–778, [https://doi.org/10.1175/1520-0485\(1998\)028<0756:OTROTA>2.0.CO;2](https://doi.org/10.1175/1520-0485(1998)028<0756:OTROTA>2.0.CO;2), 1998.
- Galbraith, E. and de Lavergne, C.: Response of a comprehensive climate model to a broad range of external forcings: relevance for deep ocean ventilation and the development of late Cenozoic ice ages, *Climate Dynamics*, 52, 653–679, <https://doi.org/10.1007/s00382-018-4157-8>, 2019.
- 290 Ganopolski, A. and Rahmstorf, S.: Rapid changes of glacial climate simulated in a coupled climate model., *Nature*, 409, 153–8, <https://doi.org/10.1038/35051500>, 2001.
- Gérard, J. and Crucifix, M.: Diagnosing the causes of AMOC slowdown in a coupled model: a cautionary tale, *Earth System Dynamics*, 15, 293–306, <https://doi.org/10.5194/esd-15-293-2024>, 2024.
- 295 Gregory, J. M., Saenko, O. A., and Weaver, A. J.: The role of the Atlantic freshwater balance in the hysteresis of the meridional overturning circulation, *Climate Dynamics*, 21, 707–717, <https://doi.org/10.1007/s00382-003-0359-8>, 2003.
- Gregory, J. M., Dixon, K. W., Stouffer, R. J., Weaver, A. J., Driesschaert, E., Eby, M., Fichefet, T., Hasumi, H., Hu, A., Jungclaus, J. H., Kamenkovich, I. V., Levermann, A., Montoya, M., Murakami, S., Nawrath, S., Oka, A., Sokolov, A. P., and Thorpe, R. B.: A model intercomparison of changes in the Atlantic thermohaline circulation in response to increasing atmospheric CO₂ concentration, *Geophysical Research Letters*, 32, 1–5, <https://doi.org/10.1029/2005GL023209>, 2005.
- 300



- Hawkins, E., Smith, R. S., Allison, L. C., Gregory, J. M., Woollings, T. J., Pohlmann, H., and De Cuevas, B.: Bistability of the Atlantic overturning circulation in a global climate model and links to ocean freshwater transport, *Geophysical Research Letters*, 38, 1–6, <https://doi.org/10.1029/2011GL047208>, 2011.
- 305 Held, I. M. and Soden, B. J.: Robust Responses of the Hydrological Cycle to Global Warming, *Journal of Climate*, 19, 5686–5699, <https://doi.org/10.1175/JCLI3990.1>, 2006.
- Heuzé, C.: North Atlantic deep water formation and AMOC in CMIP5 models, *Ocean Science*, 13, 609–622, <https://doi.org/10.5194/os-13-609-2017>, 2017.
- Heuzé, C. and Liu, H.: No Emergence of Deep Convection in the Arctic Ocean Across CMIP6 Models, *Geophysical Research Letters*, 51, <https://doi.org/10.1029/2023GL106499>, 2024.
- 310 Hofmann, M. and Rahmstorf, S.: On the stability of the Atlantic meridional overturning circulation, *Proceedings of the National Academy of Sciences of the United States of America*, 106, 20 584–20 589, <https://doi.org/10.1073/pnas.0909146106>, 2009.
- Hu, A., Meehl, G. A., Han, W., Timmermann, A., Otto-Bliesner, B., Liu, Z., Washington, W. M., Large, W., Abe-Ouchi, A., Kimoto, M., Lambeck, K., and Wu, B.: Role of the Bering Strait on the hysteresis of the ocean conveyor belt circulation and glacial climate stability, *Proceedings of the National Academy of Sciences of the United States of America*, 109, 6417–6422, <https://doi.org/10.1073/pnas.1116014109>, 2012.
- 315 Hu, A., Meehl, G. A., Abe-Ouchi, A., Han, W., Otto-Bliesner, B., He, F., Wu, T., Rosenbloom, N., Strand, W. G., and Edwards, J.: Dichotomy between freshwater and heat flux effects on oceanic conveyor belt stability and global climate, *Communications Earth and Environment*, 4, 1–15, <https://doi.org/10.1038/s43247-023-00916-0>, 2023.
- 320 Jackson, L. C. and Wood, R. A.: Hysteresis and Resilience of the AMOC in an Eddy-Permitting GCM, *Geophysical Research Letters*, 45, 8547–8556, <https://doi.org/10.1029/2018GL078104>, 2018.
- Jackson, L. C., Kahana, R., Graham, T., Ringer, M. A., Woollings, T., Mecking, J. V., and Wood, R. A.: Global and European climate impacts of a slowdown of the AMOC in a high resolution GCM, *Climate Dynamics*, 45, 3299–3316, <https://doi.org/10.1007/s00382-015-2540-2>, 2015.
- 325 Klockmann, M., Mikolajewicz, U., and Marotzke, J.: Two AMOC states in response to decreasing greenhouse gas concentrations in the coupled climate model MPI-ESM, *Journal of Climate*, 31, 7969–7984, <https://doi.org/10.1175/JCLI-D-17-0859.1>, 2018.
- Knorr, G. and Lohmann, G.: Rapid transitions in the Atlantic thermohaline circulation triggered by global warming and meltwater during the last deglaciation, *Geochemistry, Geophysics, Geosystems*, 8, <https://doi.org/10.1029/2007GC001604>, 2007.
- Lenton, T. M., Myerscough, R. J., Marsh, R., Livina, V. N., Price, A. R., and Cox, S. J.: Using GENIE to study a tipping point in the climate system, *Philosophical Transactions of the Royal Society A: Mathematical, Physical and Engineering Sciences*, 367, 871–884, <https://doi.org/10.1098/rsta.2008.0171>, 2009.
- 330 Levang, S. J. and Schmitt, R. W.: What causes the AMOC to weaken in CMIP5?, *Journal of Climate*, 33, 1535–1545, <https://doi.org/10.1175/JCLI-D-19-0547.1>, 2020.
- Lique, C. and Thomas, M. D.: Latitudinal shift of the Atlantic Meridional Overturning Circulation source regions under a warming climate, *Nature Climate Change*, 8, 1013–1020, <https://doi.org/10.1038/s41558-018-0316-5>, 2018.
- 335 Lique, C., Johnson, H. L., and Plancherel, Y.: Emergence of deep convection in the Arctic Ocean under a warming climate, *Climate Dynamics*, 50, 3833–3847, <https://doi.org/10.1007/s00382-017-3849-9>, 2018.
- Lohmann, J., Dijkstra, H. A., Jochum, M., Lucarini, V., and Ditlevsen, P. D.: Multistability and intermediate tipping of the Atlantic Ocean circulation, *Science Advances*, 10, <https://doi.org/10.1126/sciadv.adi4253>, 2024.



- 340 Manabe, S. and Stouffer, R. J.: Two Stable Equilibria of a Coupled Ocean-Atmosphere Model, [https://doi.org/10.1175/1520-0442\(1993\)006<0175:COSEOA>2.0.CO;2](https://doi.org/10.1175/1520-0442(1993)006<0175:COSEOA>2.0.CO;2), 1988.
- Mecking, J. V., Drijfhout, S. S., Jackson, L. C., and Graham, T.: Stable AMOC off state in an eddy - permitting coupled climate model, *Climate Dynamics*, 47, 2455–2470, <https://doi.org/10.1007/s00382-016-2975-0>, 2016.
- Oka, A., Hasumi, H., and Abe-Ouchi, A.: The thermal threshold of the Atlantic meridional overturning circulation and its control by wind stress forcing during glacial climate, *Geophysical Research Letters*, 39, 1–6, <https://doi.org/10.1029/2012GL051421>, 2012.
- 345 Oka, A., Abe-Ouchi, A., Sherriff-Tadano, S., Yokoyama, Y., Kawamura, K., and Hasumi, H.: Glacial mode shift of the Atlantic meridional overturning circulation by warming over the Southern Ocean, *Communications Earth and Environment*, 2, 1–8, <https://doi.org/10.1038/s43247-021-00226-3>, 2021.
- Pan, R., Shu, Q., Wang, Q., Wang, S., Song, Z., He, Y., and Qiao, F.: Future Arctic Climate Change in CMIP6 Strikingly Intensified by NEMO-Family Climate Models, *Geophysical Research Letters*, 50, 1–10, <https://doi.org/10.1029/2022GL102077>, 2023.
- Pöppelmeier, F., Scheen, J., Jeltsch-Thömmes, A., and F. Stocker, T.: Simulated stability of the Atlantic Meridional Overturning Circulation during the Last Glacial Maximum, *Climate of the Past*, 17, 615–632, <https://doi.org/10.5194/cp-17-615-2021>, 2021.
- Rahmstorf, S.: Bifurcations of the Atlantic thermohaline circulation in response to changes in the hydrological cycle, *Nature*, 378, 145–149, <https://doi.org/10.1038/378145a0>, 1995.
- 355 Rahmstorf, S., Crucifix, M., Ganopolski, A., Goosse, H., Kamenkovich, I., Knutti, R., Lohmann, G., Marsh, R., Mysak, L. A., Wang, Z., and Weaver, A. J.: Thermohaline circulation hysteresis: A model intercomparison, *Geophysical Research Letters*, 32, L23 605, <https://doi.org/10.1029/2005GL023655>, 2005.
- Roquet, F., Madec, G., Brodeau, L., and Nycander, J.: Defining a simplified yet "Realistic" equation of state for seawater, *Journal of Physical Oceanography*, 45, 2564–2579, <https://doi.org/10.1175/JPO-D-15-0080.1>, 2015.
- 360 Schmittner, A., Yoshimori, M., and Weaver, A. J.: Instability of glacial climate in a model of the ocean-atmosphere-cryosphere system, *Science*, 295, 1489–1493, <https://doi.org/10.1126/science.1066174>, 2002.
- Sgubin, G., Swingedouw, D., Drijfhout, S., Mary, Y., and Bennabi, A.: Abrupt cooling over the North Atlantic in modern climate models, *Nature Communications*, 8, 14 375, <https://doi.org/10.1038/ncomms14375>, 2017.
- Stocker, T. F. and Schmittner, A.: Influence of CO₂ emission rates on the stability of the thermohaline circulation, *Nature*, 388, 862–865, <https://doi.org/10.1038/42224>, 1997.
- 365 Stocker, T. F. and Wright, D. G.: Rapid transitions of the ocean's deep circulation induced by changes in surface water fluxes, *Nature*, 351, 729–732, <https://doi.org/10.1038/351729a0>, 1991.
- Stommel, H.: Thermohaline Convection with Two Stable Regimes of Flow, *Tellus*, 13, 224–230, <https://doi.org/10.1111/j.2153-3490.1961.tb00079.x>, 1961.
- 370 Stouffer, R. J. and Manabe, S.: Equilibrium response of thermohaline circulation to large changes in atmospheric CO₂ concentration, *Climate Dynamics*, 20, 759–773, <https://doi.org/10.1007/s00382-002-0302-4>, 2003.
- Treguier, A. M., De Boyer Montégut, C., Bozec, A., Chassignet, E. P., Fox-Kemper, B., McC Hogg, A., Iovino, D., Kiss, A. E., Le Sommer, J., Li, Y., Lin, P., Lique, C., Liu, H., Serazin, G., Sidorenko, D., Wang, Q., Xu, X., and Yeager, S.: The mixed-layer depth in the Ocean Model Intercomparison Project (OMIP): impact of resolving mesoscale eddies, *Geoscientific Model Development*, 16, 3849–3872, <https://doi.org/10.5194/gmd-16-3849-2023>, 2023.
- 375 van Westen, R. M. and Dijkstra, H. A.: Asymmetry of AMOC Hysteresis in a State-Of-The-Art Global Climate Model, *Geophysical Research Letters*, 50, <https://doi.org/10.1029/2023GL106088>, 2023.



- Weaver, A. J., Eby, M., Kienast, M., and Saenko, O. A.: Response of the Atlantic meridional overturning circulation to increasing atmospheric CO₂: Sensitivity to mean climate state, *Geophysical Research Letters*, 34, 1–5, <https://doi.org/10.1029/2006GL028756>, 2007.
- 380 Weaver, A. J., Sedláček, J., Eby, M., Alexander, K., Crespin, E., Fichet, T., Philippon-Berthier, G., Joos, F., Kawamiy, M., Matsumoto, K., Steinacher, M., Tachiiri, K., Tokos, K., Yoshimori, M., and Zickfeld, K.: Stability of the Atlantic meridional overturning circulation: A model intercomparison, *Geophysical Research Letters*, 39, 1–8, <https://doi.org/10.1029/2012GL053763>, 2012.
- Weiffenbach, J. E., Baatsen, M. L., Dijkstra, H. A., Von Der Heydt, A. S., Abe-Ouchi, A., Brady, E. C., Chan, W. L., Chandan, D., Chandler, M. A., Contoux, C., Feng, R., Guo, C., Han, Z., Haywood, A. M., Li, Q., Li, X., Lohmann, G., Lunt, D. J., Nisancioglu, K. H., Otto-Bliesner, B. L., Peltier, W. R., Ramstein, G., Sohl, L. E., Stepanek, C., Tan, N., Tindall, J. C., Williams, C. J., Zhang, Q., and Zhang, Z.: Unraveling the mechanisms and implications of a stronger mid-Pliocene Atlantic Meridional Overturning Circulation (AMOC) in PlioMIP2, *Climate of the Past*, 19, 61–85, <https://doi.org/10.5194/cp-19-61-2023>, 2023.
- 385 Weijer, W., Cheng, W., Garuba, O. A., Hu, A., and Nadiga, B. T.: CMIP6 Models Predict Significant 21st Century Decline of the Atlantic Meridional Overturning Circulation, *Geophysical Research Letters*, 47, <https://doi.org/10.1029/2019GL086075>, 2020.
- 390 Willeit, M. and Ganopolski, A.: PALADYN v1.0, a comprehensive land surface-vegetation-carbon cycle model of intermediate complexity, *Geoscientific Model Development*, 9, 3817–3857, <https://doi.org/10.5194/gmd-9-3817-2016>, 2016.
- Willeit, M., Ganopolski, A., Robinson, A., and Edwards, N. R.: The Earth system model CLIMBER-X v1.0 – Part 1: Climate model description and validation, *Geoscientific Model Development*, 15, 5905–5948, <https://doi.org/10.5194/gmd-15-5905-2022>, 2022.
- Willeit, M., Ganopolski, A., Edwards, N. R., and Rahmstorf, S.: Surface buoyancy control of millennial-scale variations of the Atlantic meridional ocean circulation, *Climate of the Past Discussions*, 20, 1–27, <https://doi.org/10.5194/egusphere-2024-819>, 2024.
- 395 Zhang, X., He, J., Zhang, J., Polyakov, I., Gerdes, R., Inoue, J., and Wu, P.: Enhanced poleward moisture transport and amplified northern high-latitude wetting trend, *Nature Climate Change*, 3, 47–51, <https://doi.org/10.1038/nclimate1631>, 2013.
- Zhang, X., Lohmann, G., Knorr, G., and Purcell, C.: Abrupt glacial climate shifts controlled by ice sheet changes, *Nature*, 512, 290–294, <https://doi.org/10.1038/nature13592>, 2014.
- 400 Zhang, X., Knorr, G., Lohmann, G., and Barker, S.: Abrupt North Atlantic circulation changes in response to gradual CO₂ forcing in a glacial climate state, *Nature Geoscience*, 10, 518–523, <https://doi.org/10.1038/ngeo2974>, 2017.
- Zhang, Z., Li, X., Guo, C., Helge Otterä, O., Nisancioglu, K. H., Tan, N., Contoux, C., Ramstein, G., Feng, R., Otto-Bliesner, B. L., Brady, E., Chandan, D., Richard Peltier, W., Baatsen, M. L., Von Der Heydt, A. S., Weiffenbach, J. E., Stepanek, C., Lohmann, G., Zhang, Q., Li, Q., Chandler, M. A., Sohl, L. E., Haywood, A. M., Hunter, S. J., Tindall, J. C., Williams, C., Lunt, D. J., Chan, W. L., and Abe-Ouchi, A.: Mid-Pliocene Atlantic Meridional Overturning Circulation simulated in PlioMIP2, *Climate of the Past*, 17, 529–543, <https://doi.org/10.5194/cp-17-529-2021>, 2021.
- 405